The Efficiency of Dodecafluoro-2-Methylpentan-3-One on Suppressing the Lithium Ion Battery Fire

The efficiency of dodecafluoro-2-methylpentan-3-one on suppressing the lithium ion battery fire

Qingsong Wang*
State Key Laboratory of Fire Science, University of Science and Technology of China, Hefei 230026, China
Collaborative Innovation Center for Urban Public Safety, Anhui Province, Hefei 230026, P.R. China
pinew@ustc.edu.cn

Ke Li
China Electric Power Research Institute, Haidian District, Beijing 100192, China
like@epri.sgcc.com.cn

Yu Wang
School of Engineering, BRE Centre for Fire Safety Engineering, University of Edinburgh, Edinburgh EH9 3JL, United Kingdom
ywang232@foxmail.com

Haodong Chen
State Key Laboratory of Fire Science, University of Science and Technology of China, Hefei 230026, China
linghao@ustc.edu.cn

Qiangling Duan
State Key Laboratory of Fire Science, University of Science and Technology of China, Hefei 230026, China
duanql@ustc.edu.cn

Jinhua Sun*
State Key Laboratory of Fire Science, University of Science and Technology of China, Hefei 230026, China
sunjh@ustc.edu.cn

* Tel.: +86 551 6360 6455; fax: +86 551 6360 1669; E-mail address: sunjh@ustc.edu.cn(J.Sun); pinew@ustc.edu.cn (Q. Wang)

ABSTRACT

To investigate the efficiency of dodecafluoro-2-methylpentan-3-one (C_6F-ketone) extinguishing agent on suppressing the lithium titanate battery fire, an experimental system was devised to implement suppression test. One 5 kW electric heater was placed at the bottom of the battery to cause the thermal runaway. The extinguishing agents of CO_2 and C_6F-ketone with different pressures were performed to suppress lithium ion battery fire. The temperatures of the battery and the flame, the ignition time, the release time of the agent, the release pressure of the agent, the time to extinguish the fire, the battery mass loss and the mass of used agent were obtained and compared in different aspects. The experimental results reveal that the lithium titanate battery fire can be suppressed by C_6F-ketone withing 30 s; the results further show that CO_2 is incapable of fully extinguishing the flame over the full duration of the test carried out. Therefore, C_6F-ketone extinguishing agent is a good candidate to put down the lithium ion battery fire.

INTRODUCTION

Lithium ion batteries (LIBs) are currently the predominant power source for portable electronics and expectedly for electric vehicles in the near future because of their high energy density, long lifespan, no memory effect, and environmental friendless[1]. A large number of researchers have investigated the principle and safe application of lithium ion batteries [2-10]. However, the fire hazards associated with large scale lithium ion battery still occur frequently. According to incomplete statistics, there were about 37 fire accidents of the large scale lithium-ion battery in 2016 in China. Thus, some previous experimental and theoretical work was conducted to study the fire hazard of lithium ion batteries. Wang et al.[11-16] studied the thermal runaway triggered fire and explosion of the lithium-ion battery. Andersson et al.[17] investigated the fire emissions from lithium ion batteries. Ribiere et al.[18] quantified thermal and toxic threat parameters of lithium ion batteries. In their studies, different types of battery cells were burnt and the emission of fluorine and/or phosphorous containing species was quantified. Fourier Transform

infrared spectroscopy (FTIR) instrument was employed to measure HF, POF_3, PF_5 and other toxic gases. The result can be obtained that, without any suppression, the combustion of a commercial electrolyte tested alone in a pool burning mode by means of the PFA apparatus entailed the release of nearly the total equivalent mass of HF (~98%). Actually, as the electrolyte contact with water, the hydrolysis reaction is happened and HF is created. Due to Ribiere's work, it can be infer that water as an agent do no help to creating more HF gases in lithium ion battery fire. In addition, Mikolajczak et al. [19] conducted the lithium ion batteries hazard by researching and assessing its safety. The lithium ion technology applications, lithium ion battery failures modes, life cycles of lithium ion cells, lithium ion fire hazard assessment and lithium ion fire hazard gap analysis were studied and analyzed in detail.

However, the studies regarding the selection of suppressants for use in lithium ion battery fires are few reported. The National Technical Information Service (NTIS) [20, 21] assessed lithium ion cells flammability and conducted fire suppression tests. In their work, different Halon products, including Halon 1301, 1211 and etc., were applied to investigate the suppression effects on the battery flame. Their results show that the Halon can suppress the battery fire basically, but after the application of Halon had ceased, the temperature of battery cell still increases. It was considered that the agent entering the inside of the cell was very hard because of the structure of the battery, so the internal reaction was still going on. Due to the Stockholm Convention, the use of Halon has been absolutely forbidden over the world since 2010. However, the previous research is still of valuable reference. The National Fire Protection Association (NFPA) [22] provided a technical report on using water as the fire extinguishing agent to deal with battery fires involving electric vehicles.

The results indicated it required at least 6 minutes of continuous fighting to put out the fire. It was a particular situation that the power was cut off, while water may burn the circuit and cause an electrical fire in some cases. There were numerous agencies claim no water was used in any lithium ion battery fire. The French aviation accident investigator, BEA, affirmed that throwing the water on a lithium ion battery fire can put out the flames, however, this could revive the fire and made its extinction more difficult, due to the release of hydrogen generated by the reduction of lithium in the water [23]. And research from the US National Renewable Energy Laboratories indicated that the only extinguisher that will work on a Lithium-ion Battery fire is a class D fire extinguisher or dry sand or dry table Salt [24]. Due to the electrical nature of battery packs, particularly the high voltages associated with large format battery packs, conductive suppression agents cannot work very well. Environmental-friendly and effective suppressants used for putting down the battery fire still need to be found.

Dodecafluoro-2-methylpentan-3-one (C_6F-ketone) is a next generation of clean agent Halon alternative [25]. It combines excellent suppression performance as well as an outstanding environmental profile. C_6F-ketone has zero ozone depletion potential, a global warming potential of one, a five-day atmospheric lifetime, and a large margin of safety for occupied spaces. It is electrically non-conducting in both liquid and gaseous states as well as vaporized cooling after suppressing, which means it has potential abilities to extinguish the battery fire. The properties of C_6F-ketone are listed in Table 1 [28]. Nevertheless, little is known about the efficiency of C_6F-ketone for battery fire. Therefore, in the present work, an experimental system was designed and built to perform the extinguishing test. The full-scale fire suppression tests were performed to evaluate the extinguishing efficiency of C_6F-

ketone on battery fire. The results are intended to provide some knowledge for battery fire suppression.

EXPERIMENTAL

An experimental system was built to perform the extinguish test as shown in Fig. 1. The system primarily consists of agent storage tank, pipelines, nozzle, battery fire source, cupboard and etc. The cupboard length, width and height are 1320 mm, 1000 mm and 2200 mm, respectively. In the cupboard, three partitions were used to separate the space into four layers. The battery can be placed in any layer in the experiment to simulate the real fire cases. Two vertical pipelines were set up in the opposite angles used to release agent. There were several release holes at the top of the cabinet with 8 mm in diameter. The fire extinguishing agent storage tank was connected to the vertical pipeline with the soft pipeline, and the volume of the tank was 10.5 L. Four glass windows were set up in the side walls and the front doors were used to view the experimental process. The combustion gases and extinguish agent were collected and ventilated to the outside by the fan after the experiment [26]. The batteries were fixed on a supporter in the middle layer of the cupboard, and a 5 kW electric heater was placed under the battery to ignite the battery, as shown in Fig. 2. The distance from the heater surface to the battery bottom surface was 55 mm. Seven K-type thermocouples (TC) were located around the battery to measure the battery surface temperature and the flame temperature. As shown in Fig. 2, two thermocouples, TC0 and TC6, were used to detect the flame temperatures, located 325 mm and 380 mm from the anode and cathode tab, respectively.

The experimental suppression design was based on the NFPA 2001: Standard on Clean Agent Fire Extinguishing Systems. The amount of C_6F-ketone agent required to achieve the design concentration shall be calculated from the following formula[27]:

$$W = \frac{V}{S}\left(\frac{C}{100-C}\right) \quad (1)$$

$$S = 0.000275T + 0.066054 \quad (2)$$

where W is the weight of clean agent, V is the net volume of hazard, S is the specific volume of the superheated agent vapor at 1 atmosphere, C is agent design concentration (volume percent), and T is the minimum anticipated temperature of the protected volume, respectively.

The weight of clean agent and agent design concentration satisfy these standard requirements. A total of 6 kg C_6F-ketone was packed into the tank first, and then the nitrogen was pressed into the tank with a pressure of 1.0 MPa or 1.5 MPa. The weight was measured before and after the experiments and then the released agent can be calculated.

Commercial lithium titanate oxide (LTO) battery was selected as the fire source. The cathode material is NMC(1:1:1) and the electrolyte is 1.0 M $LiPF_6$/EC + DEC + DMC. The capacity was 50 Ah and the voltage was 2.3 V with a diameter of 66 mm and length of 260 mm, the pressure release vent was shown in Fig. 4. The battery was charged to 100% state of charge (100% SOC) beforehand.

One experiment was performed to mitigate the battery fire using a CO_2 agent and other three suppression used C_6F-ketone. Before the experiment, the batteries were charged to the 100% state of charge, and under this condition, the batteries store the maximum energy within the capacities. The key parameters to feature the extinguish efficiency are listed in Table 2. For the Cases No. 1 to 4, single cell was heated to fire and then applied

the extinguishing agent, but the cell was placed in a battery module box in the Case 4. The module box is a container which provides a controlled environmental for working and separating the battery from receiving heat and explosion directly.

LTO battery has excellent cycle performance and stable operating voltage, but its capacity density is poor compared to other kinds of lithium ion battery, so it has been used as power sources in electric energy storage for grid rather than an electric vehicle. In a practical application, each of the LTO battery is separated by flame-retardant partition and installed in an independent module box, avoiding the chain thermal runaway in the battery cabinet. However, the potential fire risk still exists as the battery fire is not under control in time. Total flooding extinguishing system is one kind of effective fire extinguishing system within the prescribed time to the protection zone by spraying the agent. According to release a large amount of fire extinguishing agents, the chemical reaction was inhibited or oxygen was isolated or the heat was reduced in the burning fire area, then the combustion was terminated gradually which can keep for a long time. The fire did not revive again. That is the primary reason why only one LTO battery was tested in each case.

According to the study of battery combustion behavior, after the battery safety valve broke, the released material was ignited and formed a jet fire. The temperature increased above 180 ºC in a short time and the bright flame appeared, when the suppressing agent was activated manually. Besides, compared with power battery system, there was more space to install detectors in energy storage system, which mean fire signal triggering extinguishment system was also a choice in application of safety engineering.

RESULTS AND DISCUSSION

Battery fire suppression behavior

Fig. 5 displays the fire and mitigation processes of Case 1. Under the heating condition, the battery temperature increased gradually, and after 1224 s the battery safety valve was broken. Subsequently, the gases and electrolyte were spilled from the battery. The released material was ignited which formed a jet fire as shown in Fig. 5(a). The carbon dioxide was applied on the flame for several seconds, and then the flame was mitigated and transformed into a steady-state burning after 22 s. With a continuously applied carbon dioxide, the flame decreased slowly as shown in Fig. 5(d) and (e). Due to the cooling efficiency of the carbon dioxide, the steam congealed to ice attached to the pipe and the agent flow decreased. While the flammable gases were ejected continuously from the cell, the flame grew up. The gate of the cupboard was opened and hand extinguisher of carbon dioxide was used to put out the fire directly. Therefore, the battery fire is difficult to put down with CO_2 total flooding system. The result indicates that the carbon dioxide is not appropriate to be used to suppress the lithium titanium battery fire.

Fig. 6 shows the fire and suppression processes of Case 2. Firstly the battery safety valve was also broken under the heating condition after 882 s. The gases and electrolyte were spilled or dropped from the battery. The released electrolyte was ignited by the heater and then the jet gases as shown in Fig. 6(a). The C_6F-ketone was applied on the flame at 4 s after ignition. Then the flame struggled to extinguish and the flame area decreased in few seconds, and it was extinguished in 15 s finally. To avoid the fire revived again, the agent released last 50 s. With lower pressure and less time compared to the carbon dioxide, the fire was extinguished, which indicated that the C_6F-ketone can be used to suppress the LTO battery fire.

Another experiment was performed to investigate the repeatability and the extinguishing process, as shown in Fig. 7. In Case 3, the pressure of agent was adjusted to 1.0 MPa, with lower maintenance costs and efficiency of suppressing compared with Case 2. The battery also underwent a heated process and ejected gases at 1079 s, and a strong jet fire was formed. After the spray of the agent on the fire, the flame was put down after 23 s. To avoid the fire revived again, the agent released last 40 s. The results suggest that C_6F-ketone has a good performance in putting out the LTO battery fire with lower pressure under this condition.

To investigate the extinguishing effects of C_6F-ketone on battery fire packed in module box, the experiment Case 4 was designed and conducted.

The experimental apparatus of case 4 is shown in Fig. 8. The battery module box was designed and built to store battery pack for commercial purposes originally. The battery pack box only consisted the sample used in the test, and one sidewall of the box was taken away to let the extinguishing agent permeate into the box. The LTO battery fire extinguishing process using C_6F-ketone in Case 4 is shown in Fig. 9. The heated process was similar to that of experiment Cases 1-3. After the spray of the agent on the fire, the flame was put down after 24 s. To avoid the fire revived again, the agent released last 45 s. The time of ignition for Case 4 is shorter than the other three cases, only cost 859 s, because the battery was heated in a narrow space, and the chemical reaction inside the battery vigorously in return, which demonstrated that the battery may get thermal runaway more likely. Therefore, the heat elimination was very important to the battery pack inside the box in the practical application.

Actually, the C_6F-Ketone is not an agent specially developed for a lithium ion battery fire, while the efficiency of C_6F-Ketone extinguish battery fire by thermal decomposition and reaction with chain-carrier radicals. Fig. 10 presents the reaction pathways of C_6F-Ketone decomposition. When the activity of free radicals generated by the decomposition extinguishing agent is sprayed to the protection zone, flame or fire extinguishing agent contact hot surfaces, the radical chain reaction seize combustion generated active substances, destruction combustion process chain transfer, and ultimately achieve the purpose of extinguishing the ways a chemical fire, cooled, diluted or cut off the air and other physical effect is minimal [29].

Temperature distribution of the battery

The temperature of the cell and the flame are the most persuasive data to demonstrate the features of the battery before and after thermal runaway. Seven K-type thermocouples, numbered from TC0 to TC6, were fixed around the battery to measure temperatures of the battery surface and the flame. Fig. 11 shows the temperature of cell and flame before and after applying the extinguishing agent in the experiment Case 1.

The temperature of the cell grew quickly once the electric heater began to work, while the air temperature increased relatively slowly by contrast due to thermodynamic parameters of the cell. After applying the agent, both the battery temperature and the air temperature around the cell decreased markedly within a very short time, then fluctuated near a value on average. As shown in Fig. 11, at about 1224 s, the temperature of the cathode tab rose perpendicularly from 90.3 °C to 175 °C. The flame temperature reached 362 °C near the cathode tab as well. As soon as applying the agent, the temperature at

cathode tab decreased to 132 °C, while the temperature detected by TC6 was equal to ambient because the flammable gases ejected continuously from the battery and flame burnt weakly after the agent was applied, in the meanwhile TC6 was not in the zoom of flame. The violent exothermic chemical reaction was still ongoing in the battery after the carbon dioxide was applied. The cell surface temperature variations of different positions were almost identical as shown in Fig. 11, which demonstrates that the chemical reaction was uniform inside the battery. The difference in the temperature curve of the cathode tab is that there was no sudden temperature rise in anode tab and around since no flammable gases and electrolyte were spilled from the battery anode.

Generally, the temperature of the cell rose rapidly once the electric heater began to work. On the contrary, the flame temperature increased relatively slowly. After applying the agent, both the cell temperature and the air temperature around the cell started to drop within a very short time, which proves that the flame was controlled completely by the extinguishing agent. As shown in Fig. 12, at about 882 s, the temperature of the anode tab and air near the anode rose perpendicularly from 121.2 °C to 175 °C and 52 °C to 573.1 °C, respectively. As soon as applying the C_6F-ketone, the temperature at anode tab and the flame temperature decreased to 89 °C and 38 °C within seconds. The cell surface temperature variations of different positions were almost the same as well, which demonstrates that the chemical reaction is continuing in the battery. There is no sudden temperature rise in cathode tab and around because no flammable gases and electrolyte were spilled from the battery cathode as the same reason in Case 1.

Fig. 13 presents the temperature of the cell before and after applying the extinguishing agent of experiment Case 3. As shown in Fig. 13, the insulated skin of the

cell melted approximately after 360 s, which produced a mass of smoke. The flammable gases and electrolyte were spilled from the cathode of the battery in Case 3. Therefore the cathode tab temperature was 32 °C higher than the anode tab before the thermal runaway. The battery temperature rebound after stopping the application of extinguishing agent and then decreased gradually to the room temperature.

The cell temperature of experiment Case 4 is shown in Fig. 14. The cell center temperature rose more rapidly than those at tabs, which was caused by the battery heated in a narrow space and the nonuniformity of the chemical reactions inside. The high temperature of battery reached 197.8 °C, and at the same time, the cell went to thermal runaway.

Comparison of suppression efficiency

The temperature of cell and air around before and after in 600 s applying the extinguishing agent of the experiment from Case 1 to Case 4 are shown in Fig. 15. The temperature variations were very similar in Case 1 and Case 2, but the result turned to be different. In Case 1, the flame was weak and the temperature still rose 40 ºC after the agent was applied, compared with the condition the battery started thermal runaway. While the fire was suppressed and the temperature was equal to prior to the application of suppressing agent in Case 2. Considering the mechanism of CO_2 and C_6F-ketone extinguish the fire, both agents extinguished the fire by physically attacking all three points of the fire triangle. The suppression process was aided by a decrement in the concentration of oxygen and gasified fuel in the flame area. At the same time, agents did provide some cooling in the fire zone to assist the extinguishing process. While compared to the CO_2, C_6F-ketone

additionally involves the combustion reaction to complete the flame termination progress. Thus, it is necessary to figure out the cooling ability and chemical inhibition which played a dominant role in the extinguishing experiment using C_6F-ketone.

A simple model was built to study the efficiency of cooling ability of CO_2 and C_6F-ketone when the agent was applied to a battery fire. Due to many researchers' work, a 1D computational model was developed and compared with an analytical approach and a three-dimensional (3D) computational fluid dynamics (CFD) simulation. It was demonstrated that the 1D model was sufficient to predict the temperature distribution of the lithium-ion battery. Actually, it is of great challenge to simulate a fire or the gas in a flame, here several assumptions were made in the simulation as follows: the whole system consisted of the flammable gas and the battery was a lumped capacitance body, which signified the data of battery cooling process can be used to predict the tendency of temperature variation in the whole system; the process of the whole closet filled with agent so quickly that the time can be ignored. In a word, the heat exchanged from battery to ambient agent directly; there was no chemical reaction coupled to this progress, only the efficiency of heat transfer was studied in this model.

The cylindrical battery cell was cooled by the agent on the surface in the same proportion of room. The equations of this model are presented as follows:

$$\rho C_p \frac{\partial \boldsymbol{T}}{\partial \boldsymbol{t}} + \nabla \cdot \boldsymbol{q} = Q \tag{3}$$

$$\boldsymbol{q} = -\boldsymbol{k}\nabla \boldsymbol{T} \tag{4}$$

where C_p represents specific heat coefficient, ρ represents density, $\boldsymbol{q}$ represents heat density, Q represents heat source, $\boldsymbol{k}$ represents thermal conductivity.

In this model, conduction through a stagnant agent is the dominant transport mechanism, so the convection heat transfer is considered existing on the surface of the cupboard.

$$-\boldsymbol{n}\cdot\boldsymbol{k}\nabla\boldsymbol{T}=\boldsymbol{h}\cdot(\boldsymbol{T}_{ext}-\boldsymbol{T}) \quad (5)$$

where $\boldsymbol{k}$ represents thermal conductivity, $\boldsymbol{h}$ represents heat transfer coefficient**,** and $\boldsymbol{T}_{ext}$ is the external temperature. While on the fire side $\boldsymbol{T}_{ext}$ is equal to 25 ºC on average. The relevant parameters in this study are listed in Table 3. In our previous work (Huang et al., 2015a) as the battery went into thermal runaway, the heat release rate was 5 kW on average in the stage of stable combustion. The maximum heat source set at 5000 W.

The surface and average temperature of the battery were cooled by the agent for computational models as shown in Fig. 16. The result demonstrated that the surface of the battery was cooled down immediately while the whole body still remained at a high temperature at the beginning of the cooling process. As the reaction continued, the surface temperature effortlessly backed to the same level of the whole body, which indicated the force of natural convection and heat conduction by gas did not play a key role in the extinguishment.

Table 4 presented the surface and average temperature of the battery with different thermal loads and supplied agent for computational models. With the same thermal load, the temperature distribution with CO_2 as well as C_6F-ketone was almost identical. Though the agent physical parameters existed difference, there were several orders of magnitude of physical parameters between battery and agent. The effort of natural convection and heat conduction at the beginning played an important role in the battery cooling down the

process, while as the heat generated continuously, the difference between surface and body became small and the system turned to be uniform.

The result indicates both agents have very similar cooling ability. Thus it can be inferred the chemical inhibition ability contributed to C_6F-ketone suppressing the battery fire indirectly. That is the point why the fire had been extinguished in Case 2-4 excluding Case 1, though the temperature of these cases are very similar, for the agents have the analogous cooling and asphyxiant capabilities.

The results were compared in Fig. 15, and the temperature distribution had the same tendency, though the fire was not put out when carbon dioxide was applied for the first time. Once the C_6F-ketone was applied to fire, the temperature almost decreased to the same level as the thermal runaway occurred, while the temperature in Case 1 was a little bit higher for fire weakening. Both carbon dioxide and C_6F-ketone can cool down the whole system but carbon dioxide cannot put down the battery fire effectively. The results indicate that the extinguishment process using C_6F-ketone not only involves the heat transfer process but also couples with chemical reaction process terminating the combustion reaction. The results of simulation experiment agree with this conclusion.

According to the report by NFPA [27], as C_6F-ketone was applied to the fire with high temperature and the primary extinguishing mechanism of C_6F-ketone fluid is heat absorption, with a secondary chemical contribution from the thermal decomposition of C_6F-ketone fluid in the flame. When C_6F-ketone fluid is exposed to extremely high temperatures, the by-product HF will be formed, which means C_6F-ketone is applicable for unmanned operation, and the agent of portable extinguisher used to put down the LIB fire still needs to be found.

CONCLUSIONS

A total of four experiments were conducted to investigate the efficiency of carbon dioxide and C_6F-ketone fire extinguishing agent for the single lithium titanium battery fire suppression. The primary results are as follows:

The ignition of the flammable gases and electrolyte spilled from the battery safety valve is the main cause of lithium titanium battery fire. Strong jet fire may be formed due to the short circuit and the direct reaction between the cell anode and cathode after the melting of the separator. The temperature increased over 180 ºC in a short time and the suppressing agent was activated.

The lithium titanium battery fire can be extinguished by C_6F-ketone within 30 seconds, no matter if the battery is in an open or enclosure space. Physical cooling and chemical combustion reaction blocking are primary mechanisms for C_6F-ketone to extinguish battery fire.

When C_6F-ketone fluid is exposed to extremely high temperatures, the by-product HF will be formed. The agent of portable extinguisher used for putting out the LIB fire is still needed to be studied. The efficiency of the agent during the later stage of battery fire and other types of lithium ion batteries fire will be tested in future works, which might present more challenging issues for C_6F-ketone.

ACKNOWLEDGMENT

This work is supported by the National Key R&D Program of China (No.2016YFC0801505), National Natural Science Foundation of China (No. 51674228), the External Cooperation Program of BIC, CAS (No. 211134KYSB20150004) and the

Fundamental Research Funds for the Central Universities (No. WK2320000034). Dr. Q.S Wang is supported by Youth Innovation Promotion Association CAS (No.2013286).

REFERENCES

[1] Z. Wang, L. Zhou, Metal Oxide Hollow Nanostructures for Lithium‐ion Batteries, Advanced materials 24(14) (2012) 1903-1911. DOI: 10.1002/adma.201200469

[2] G.-H. Kim, K. Smith, J. Ireland, A. Pesaran, Fail-safe design for large capacity lithium-ion battery systems, J. Power Sources 210 (2012) 243-253. https://doi.org/10.1016/j.jpowsour.2012.03.015

[3] E. Sahraei, J. Meier, T. Wierzbicki, Characterizing and modeling mechanical properties and onset of short circuit for three types of lithium-ion pouch cells, J. Power Sources 247 (2014) 503-516. https://doi.org/10.1016/j.jpowsour.2013.08.056

[4] M. Nakayama, K. Iizuka, H. Shiiba, S. Baba, M. Nogami, Asymmetry in anodic and cathodic polarization profile for LiFePO4 positive electrode in rechargeable Li ion battery, J. Ceram. Soc. Jpn. 119(1393) (2011) 692-696. http://doi.org/10.2109/jcersj2.119.692

[5] P. Röder, N. Baba, K.A. Friedrich, H.D. Wiemhöfer, Impact of delithiated Li0FePO4 on the decomposition of LiPF6-based electrolyte studied by accelerating rate calorimetry, J. Power Sources 236(0) (2013) 151-157. https://doi.org/10.1016/j.jpowsour.2013.02.044

[6] T. Wakao, T. Gunji, A.J. Jeevagan, Y. Mochizuki, S. Kaneko, K. Baba, M. Watanabe, Y. Kanda, K. Murakami, M. Omura, G. Kobayashi, F. Matsumoto, Stable Charge/Discharge Cycle Performance of a LiFePO4 Cathode Prepared With a Carboxymethyl Cellulose Binder, Ecs. Transactions. 58(25) (2014) 19-25. doi: 10.1149/05825.0019ecst

[7] C. Capasso, O. Veneri, Experimental analysis on the performance of lithium based batteries for road full electric and hybrid vehicles, Appl. Energ. 136 (2014) 921-930. https://doi.org/10.1016/j.apenergy.2014.04.013

[8] J. Lamb, C.J. Orendorff, L.A.M. Steele, S.W. Spangler, Failure propagation in multi-cell lithium ion batteries, J. Power Sources 283 (2015) 517-523. https://doi.org/10.1016/j.jpowsour.2014.10.081

[9] N. Omar, M.A. Monem, Y. Firouz, J. Salminen, J. Smekens, O. Hegazy, H. Gaulous, G. Mulder, P. Van den Bossche, T. Coosemans, Lithium iron phosphate based battery–assessment of the aging parameters and development of cycle life model, Appl. Energ. 113 (2014) 1575-1585. https://doi.org/10.1016/j.apenergy.2013.09.003

[10] F. Ren, T. Cox, H. Wang, Thermal runaway risk evaluation of Li-ion cells using a pinch–torsion test, J. Power Sources 249 (2014) 156-162. https://doi.org/10.1016/j.jpowsour.2013.10.058

[11] Q.S. Wang, P. Ping, J.H. Sun, C.H. Chen, Improved thermal stability of lithium ion battery by using cresyl diphenyl phosphate as an electrolyte additive, J. Power Sources 195 (2010) 7457–7461. https://doi.org/10.1016/j.jpowsour.2010.05.022

[12] P. Ping, Q.S. Wang, J.H. Sun, H.F. Xiang, C.H. Chen, Thermal Stabilities of Some Lithium Salts and Their Electrolyte Solutions With and Without Contact to a LiFePO(4) Electrode, J. Electrochem. Soc. 157(11) (2010) A1170-A1176. doi: 10.1149/1.3473789

[13] Q.S. Wang, P. Ping, X.J. Zhao, G.Q. Chu, J.H. Sun, C.H. Chen, Thermal runaway caused fire and explosion of lithium ion battery, J. Power Sources 208 (2012) 210-224. https://doi.org/10.1016/j.jpowsour.2012.02.038

[14] P. Ping, Q.S. Wang, P.F. Huang, K. Li, J.H. Sun, D.P. Kong, C.H. Chen, Study of the fire behavior of high-energy lithium-ion batteries with full-scale burning test, J. Power Sources 285 (2015) 80-89. https://doi.org/10.1016/j.jpowsour.2015.03.035

[15] P. Huang, Q. Wang, K. Li, P. Ping, J. Sun, The combustion behavior of large scale lithium titanate battery, Sci Rep 5 (2015) 7788. doi: 10.1038/srep07788

[16] Q. Wang, Q. Sun, P. Ping, X. Zhao, J. Sun, Z. Lin, Heat transfer in the dynamic cycling of lithium–titanate batteries, Int. J. Heat Mass Tran. 93 (2016) 896-905.

[17] P. Andersson, P. Blomqvist, A. Lorén, F. Larsson, Investigation of fire emissions from Li-ion batteries, SP Technical Research Institute of Sweden2013. https://doi.org/10.1016/j.ijheatmasstransfer.2015.11.007

[18] P. Ribiere, S. Grugeon, M. Morcrette, S. Boyanov, S. Laruelle, G. Marlair, Investigation on the fire-induced hazards of Li-ion battery cells by fire calorimetry, Energ. Environ. Sci. 5(1) (2012) 5271-5280. DOI: 10.1039/C1EE02218K

[19] C. Mikolajczak, M. Kahn, K. White, R.T. Long, Lithium-ion batteries hazard and use assessment, Springer Science & Business Media2012.

[20] S.M. Summer, Flammability Assessment of Lithium-Ion and Lithium-Ion Polymer Battery Cells Designed for Aircraft Power Usage, US Department of Transportation, Federal Aviation Administration, 2010.

[21] B. Ditch, J. de Vries, Flammability characterization of lithium-ion batteries in bulk storage, FM Global2013.

[22] O.B. PARK, Best Practices for Emergency Response to Incidents Involving Electric Vehicles Battery Hazards: A Report on Full-Scale Testing Results, (2013).

[23] B.E.A, Cabin Fire during Cruise, www.bea.aero/docspa/2010/f-pk101208.en/pdf/f-pk101208.en.pdf.

[24] N.R.E.L, Safety Hazards of Batteries , http://www.nrel.gov/education/pdfs/lithium-ion_battery_safety_hazards.pdf

[25] P.E. Rivers, Advancement in sustainable fire suppression development C6F-ketone: a novel new Halon replacement alternative to HFCs and PFCs, Proceedings of the 2001 Halon Options Technical Working Conference, 2001, pp. 341-348.

[26] Q. Wang, G. Shao, Q. Duan, M. Chen, Y. Li, K. Wu, B. Liu, P. Peng, J. Sun, The efficiency of heptafluoropropane fire extinguishing agent on suppressing the lithium titanate battery fire, Fire Technology 52(2) (2016) 387-396. https://doi.org/10.1007/s10694-015-0531-9

[27] N.F.P. Association, NFPA 2001: Standard on Clean Agent Fire Extinguishing Systems, National Fire Protection Association2000.

[28] A. Kim, G. Crampton, Performance of Novec1230 in electronic facility fire protection, National Research Council Canada NRCC-53526 (2010).

[29] Xu W, Jiang Y, Ren X. Combustion promotion and extinction of premixed counterflow methane/air flames by C6F12O fire suppressant[J]. Journal of Fire Sciences, 34(4) (2016) .

Figure Captions List

Table Caption List

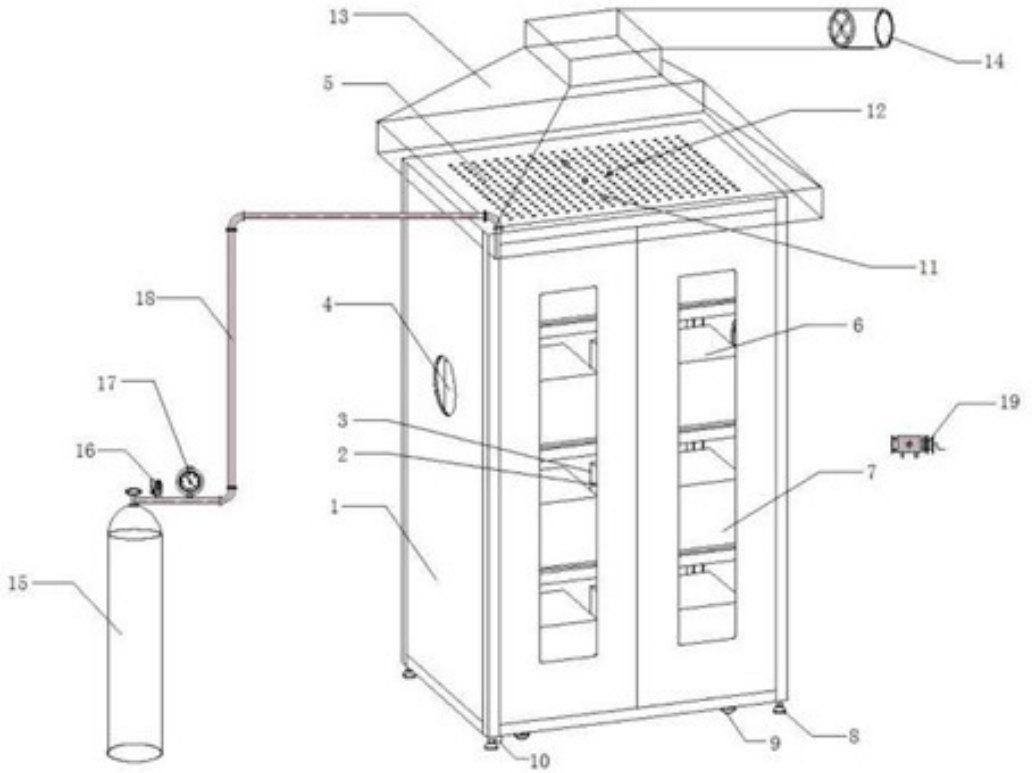

Fig. 1 The experimental apparatus, in which 1 is battery cupboard, 2 is heat source, 3 is battery supporter, 4 is sidewall window, 5 is upper ventilation hole, 6 is partition, 7 is hinged door, 8 is foot screw, 9 is wheel, 10 is vertical fire extinguishing agent release pipe, 11 is fire alarms, 12 is nozzle, 13 is exhaust fume collecting hood, 14 is explosion-proof fan, 15 is fire extinguishing agent storage tank, 16 is flow control valve, 17 is pressure gauge, 18 is high-pressure pipeline, 19 is camera.

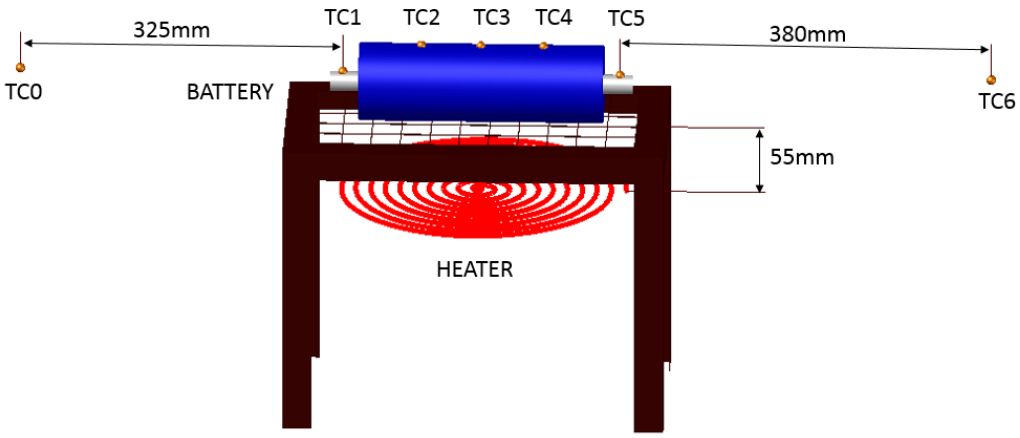

Fig. 2 The location of the battery and thermocouples in the experiment.

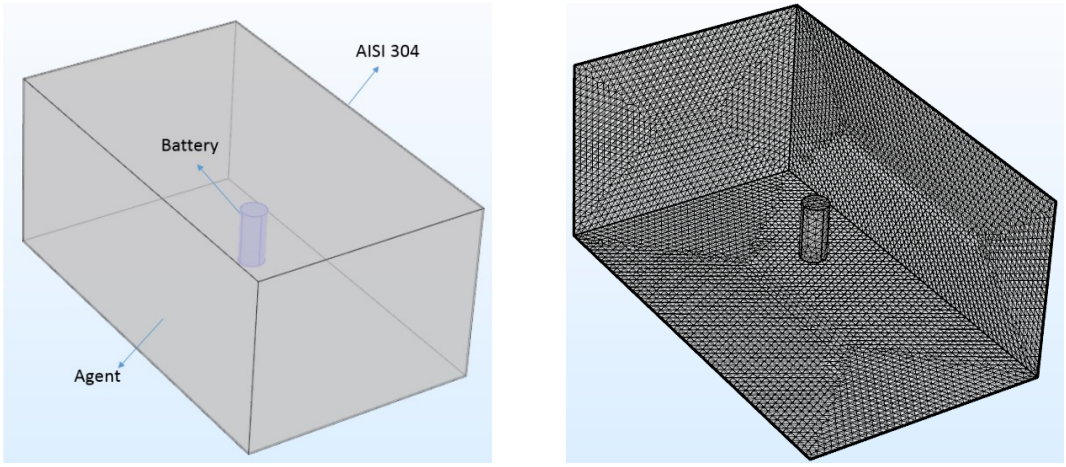

(a) spatial distribution of elements (b) the mesh

Fig. 3 Schematic diagram of simulation model

Fig. 4 The safety vent near the collector column

(a) The jet fire was formed

(b) Carbon dioxide was applied

(c) After 22s carbon dioxide was applied

(d) After 76s the flame decreased

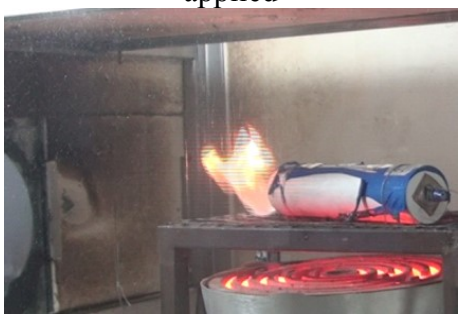

(e) After 110s

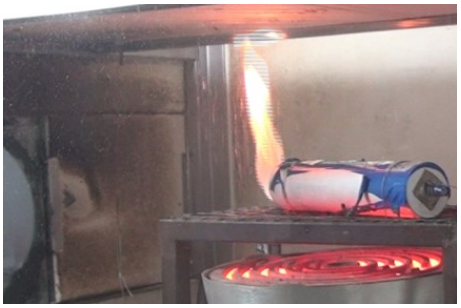

(f) The agent decreased and fire recovered（164s）

Fig. 5 The LTO battery fire extinguishing process using carbon dioxide in Case 1

(a) The dropped electrolyte was ignited

(b) 2 s after ignition

(c) The agent was applied at 4s after ignition

(d) 15 s after applied the agent the fire was put out

Fig. 6 The LTO battery fire extinguishing process using C_6F-ketone in Case 2

(a) 1079 s after oven heated the battery, the dropped electrolyte was ignited

(b) 2 s after ignition

(c) The agent was applied at 3 s after ignition

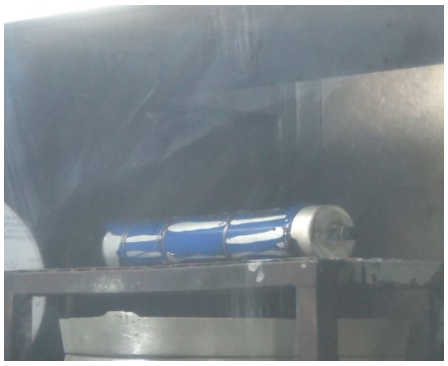

(d) 23 s after applied the agent the fire was put out

Fig. 7 The LTO battery fire extinguishing process using C_6F-ketone in Case 3

(a) Front view of the battery box (b) Side view of the battery box

Fig. 8 The experimental set up of Case 4

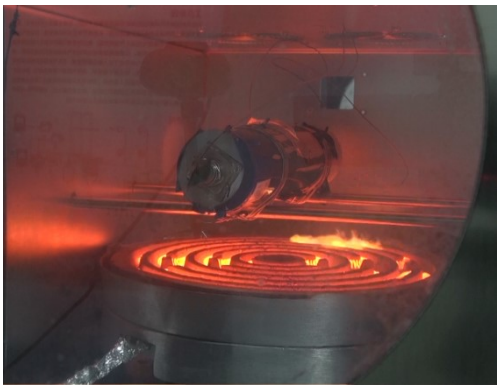

(a) 859 s after oven heated the battery, the dropped electrolyte was ignited

(b) 2 s after ignition, both cathode and anode caught on fire

(c) The agent was applied at 3 s after ignition

(d) The fire was under control, 24 s after ignition the fire was put out

Fig. 9 The LTO battery fire extinguishing process using C_6F-ketone in Case 4

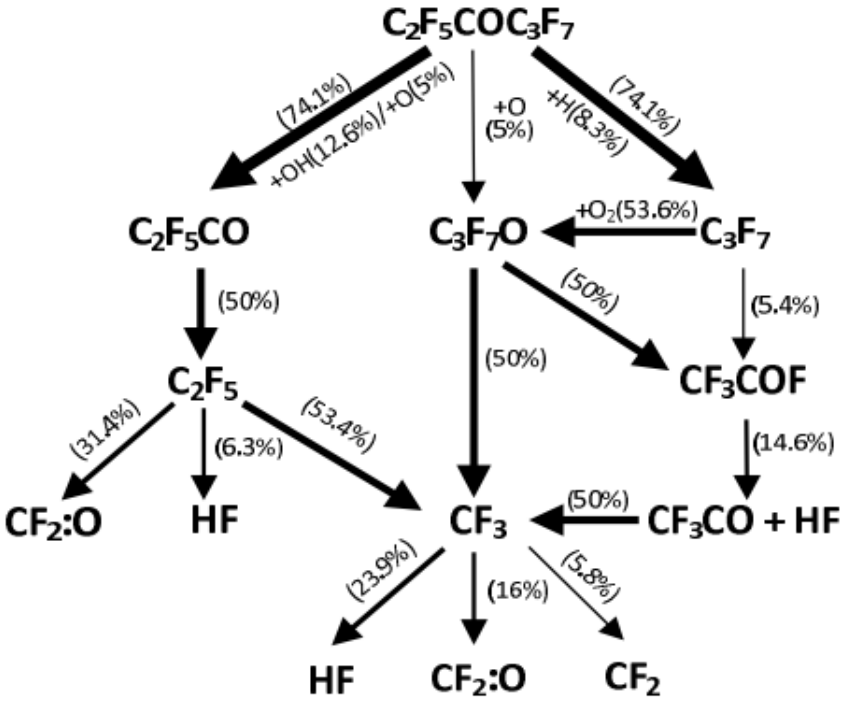

Fig. 10 Reaction pathways of C_6F-Ketone decomposition [29].

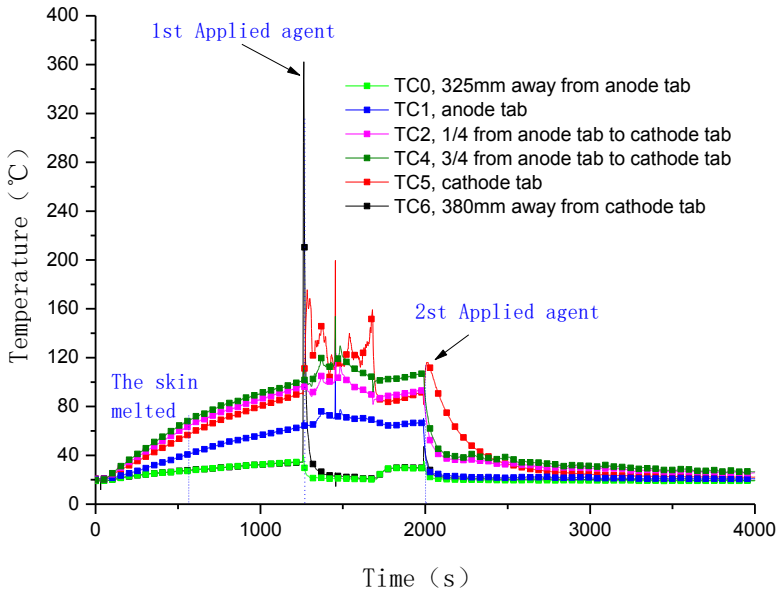

Fig. 10 Temperature of cell and air around before and after applying CO_2 agent in Case 1.

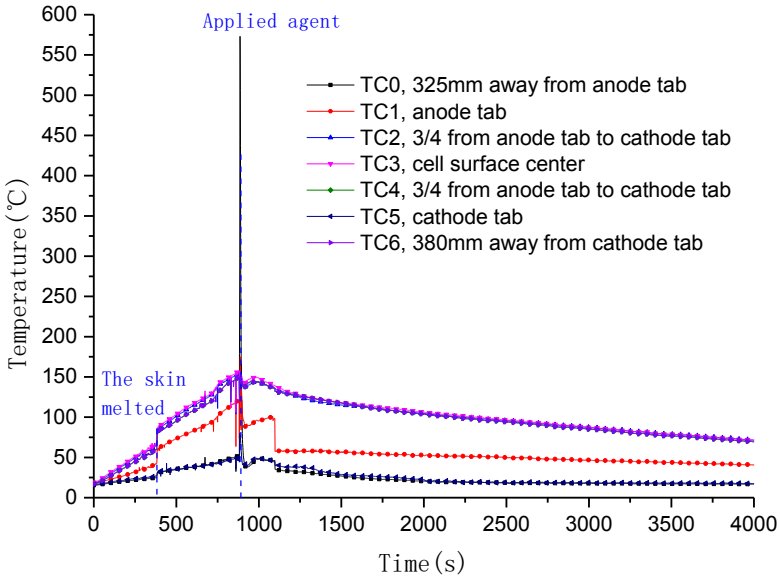

Fig. 11 Temperature of cell and air around before and after applying extinguish agent of experiment Case 2.

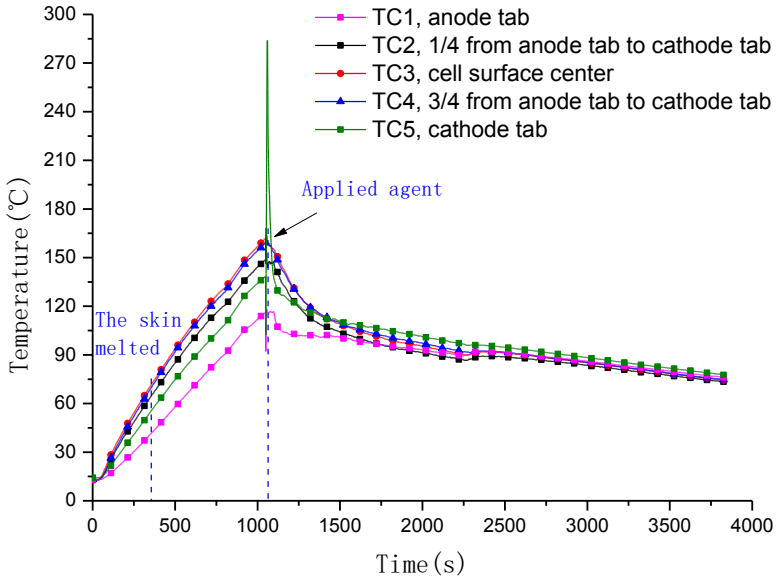

Fig. 12 Temperatures of cell and air around before and after applying extinguish agent of experiment Case 3.

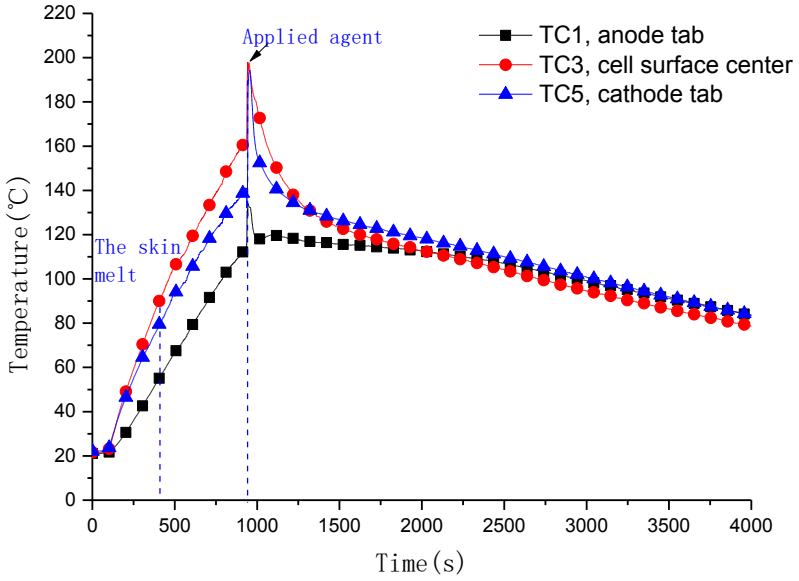

Fig. 13 Temperatures of cell and air around before and after applying extinguish agent of experiment Case 4.

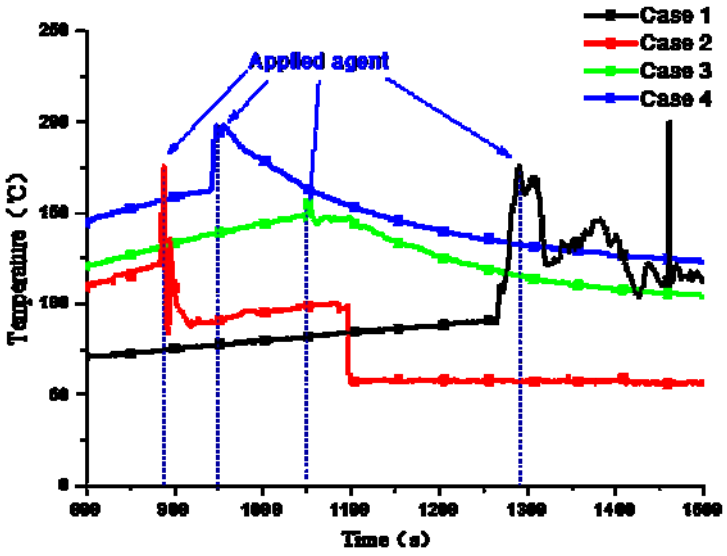

(a) the maximum temperature of the battery cell from Case 1 to Case 4

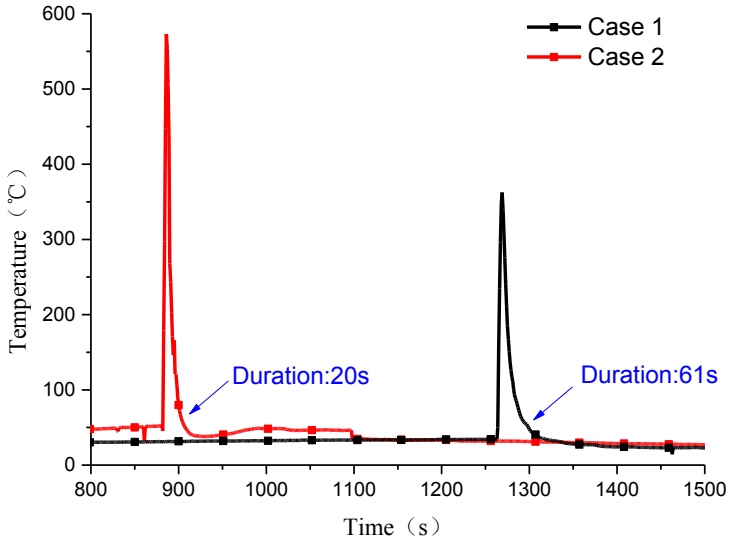

(b) the temperature of air around in Case 1 and Case 2

Fig. 14 Temperature of cell and air around before and after in 600 s applying extinguish agent of the experiment from Case 1 to Case 4.

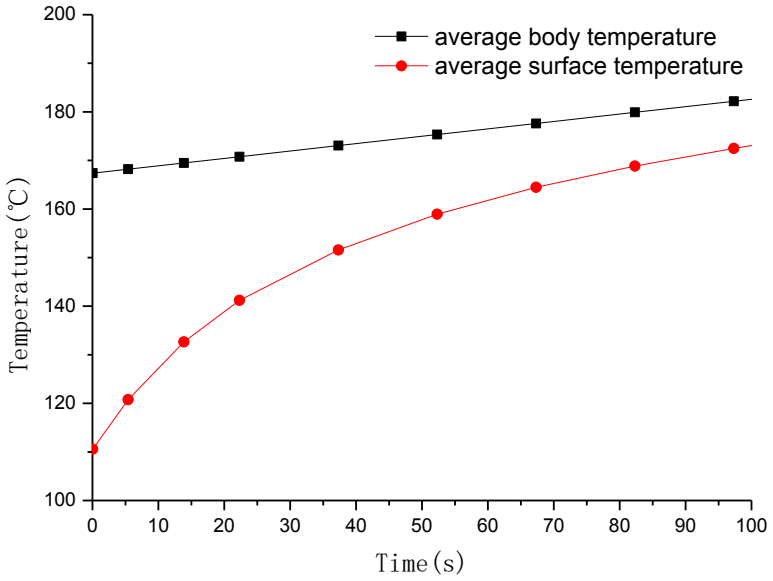

Fig. 15 Surface temperature and average temperature of the battery cooled by agent for computational models with the heat source of 500 W

Table 1. Properties of the C_6F-Ketone

Properties	C_6F-ketone
Chemical formula	$CF_3CF_2C(O)CF(CF_3)_2$
Molecular weight	316.04
Boiling point at 1 atm	49.2 ºC
Freezing point	-108.0 ºC
Critical temperature	168.7 ºC
Critical pressure	18.65 bar
Critical volume	494.5 cc/mole
Critical density	639.1 kg/m^3
Density, Sat. Liquid	1.60 g/ml
Density, Gas at 1 atm	0.0136 g/ml
Specific volume, Gas at 1 atm	0.0733 g/ml
Specific Heat, liquid	1.103kJ/kg K
Specific Heat, vapor at 1 atm	0.891kJ/kg K
Heat of vaporization at boiling point	88.0 kJ/kg
Relative dielectric strength, 1 atm(N_2=1.0)	2.3

Table 2. The summary of key extinguish parameters

Items	Case 1	Case 2	Case 3	Case 4
Conditions	Single cell	Single cell	Single cell	Single cell in box
Agent	CO_2	C_6F-ketone	C_6F-ketone	C_6F-ketone
Time to ignition (s)	1224	882	1079	859
Release pressure (MPa)	15	1.5	1.0	1.0
Release time (s)	173	50	40	45
Extinguish time (s)	N/A	15	23	24
Battery original mass(g)	1648	1645	1642	1654
Battery mass loss (g)	696	69	62	89
Loaded agent mass (kg)	40.00	4.088	4.000	6.208
Used agent mass (kg)	2.482	3.666	3.974	5.076

Table 3. Thermophysical properties of the material and initial value in the simulation

Items	Value
Specific heat coefficient of steel AISI 304 ($J \cdot kg^{-1} \cdot K^{-1}$)	477
Thermal conductivity of steel AISI 304($W \cdot m^{-1} \cdot K^{-1}$)	14.9
Density of steel AISI 304($kg \cdot m^{-3}$)	7900
Specific heat coefficient of battery ($J \cdot kg^{-1} \cdot K^{-1}$)	1605
Thermal conductivity of battery ($W \cdot m^{-1} \cdot K^{-1}$)	32
Density of battery ($kg \cdot m^{-3}$)	2285
Specific heat coefficient of CO_2 ($J \cdot kg^{-1} \cdot K^{-1}$)	851
Thermal conductivity of CO_2($W \cdot m^{-1} \cdot K^{-1}$)	0.0166
Density of CO_2 ($kg \cdot m^{-3}$)	1.773
Specific heat coefficient of C_6F-ketone ($J \cdot kg^{-1} \cdot K^{-1}$)	891
Thermal conductivity of C_6F-ketone ($W \cdot m^{-1} \cdot K^{-1}$)	0.060
Density of steel C_6F-ketone ($kg \cdot m^{-3}$)	13.6
Heat transfer coefficient	20
Ambient temperature(ºC)	25
Initial temperature of the battery (ºC)	300

Table 4. The results of simulation the heat transfer process after 100 s

Agent	Position	Temperature with different heat source power (°C)			
		10 W	100 W	500 W	5000 W
CO_2	Body	178.62	181.38	193.63	331.46
	Surface	171.21	173.97	186.21	323.86
C_6F-ketone	Body	178.28	181.02	193.24	330.60
	Surface	170.66	173.40	185.50	322.38